Dynamics of ITCZ width: Ekman processes, non-Ekman processes and links to sea-surface temperature

Michael P. Byrne*

University of St Andrews, Fife, UK and University of Oxford, Oxford, UK

Rhidian Thomas and Arnaud Czaja

Imperial College, London, UK

**Corresponding author address:* Michael P. Byrne, School of Earth & Environmental Sciences, University of St Andrews, KY16 9AL Fife, United Kingdom

E-mail: mpb20@st-andrews.ac.uk

ABSTRACT

The dynamical processes controlling the width of the intertropical convergence zone (ITCZ) are investigated using idealized simulations. ITCZ width is defined in terms of boundary-layer vertical velocity. The tropical boundary layer is approximately in Ekman balance suggesting that wind stress places a strong constraint on ITCZ width. A scaling based on Ekman balance predicts that ITCZ width is proportional to the wind stress and inversely proportional to its meridional gradient. A toy model of an Ekman boundary layer illustrates the effects of wind-stress perturbations on ITCZ width. A westerly wind perturbation widens the ITCZ whereas an easterly perturbation narrows the ITCZ. Multiplying the wind stress by a constant factor does not shift the ITCZ edge, but ITCZ width is sensitive to the latitude of maximum wind stress. Scalings based on Ekman balance cannot fully capture the behavior of ITCZ width across simulations, suggesting that non-Ekman dynamical processes need to be accounted for. An alternative scaling based on the full momentum budget explains variations in ITCZ width and highlights the importance of horizontal and vertical momentum advection. Scalings are also introduced linking ITCZ width to surface temperature. An extension to Lindzen-Nigam theory predicts that ITCZ width scales with the latitude where the Laplacian of SST is zero. The supercriticality theory of Emanuel (1995) is also invoked to show that ITCZ width is dynamically linked to boundary-layer moist entropy gradients. The results establish a dynamical understanding of ITCZ width that can be applied to interpret persistent ITCZ biases in climate models and the response of tropical precipitation to climate change.

1. Introduction

The intertropical convergence zone (ITCZ) is a planetary-scale band of low-level mass convergence and intense rainfall (Waliser and Gautier 1993). The ITCZ migrates north and south across the equator in response to seasonal changes in insolation. Given its dominant influence on tropical hydroclimate and importance for societies at low latitudes, the physical mechanisms controlling the ITCZ have received considerable attention (e.g., Philander et al. 1996; Broccoli et al. 2006; Kang et al. 2008; Frierson et al. 2013; Donohoe et al. 2013; Bischoff and Schneider 2014; Byrne and Schneider 2016a). The bulk of ITCZ research has focused on the mechanisms controlling its mean position or latitude, and these mechanisms are now well understood at least in the zonal-mean context (see reviews by Chiang and Friedman 2012; Schneider et al. 2014; Donohoe and Voigt 2017; Kang et al. 2018). By comparison, the processes determining the width of the ITCZ are relatively under-studied despite its importance for regional and global climate. Recent work has shown that ITCZ width influences global precipitation and top-of-atmosphere energy balance (Su et al. 2017; Byrne and Schneider 2018) and is dynamically linked to the poleward extent of the Hadley cell and the latitudes of the storm tracks (Watt-Meyer and Frierson 2019). Furthermore, changes in ITCZ width in response to radiative forcing are strongly anti-correlated with changes in ITCZ strength (Byrne et al. 2018), suggesting that a better understanding of the processes controlling ITCZ width could help constrain ITCZ strength and tropical rainfall intensity.

We currently lack a closed theory for ITCZ width and its response to climate perturbations. In recent years, however, progress has been made in understanding how different processes affect ITCZ width. A theory derived from atmospheric mass and moist static energy budgets shows how the ITCZ narrows or widens in response to changes in gross moist stability, cloud radiative effects, energy/moisture advection and moisture transport by transient eddies (Byrne and Schneider 2016a); other studies also identified that these processes can affect ITCZ width (Bretherton and Sobel 2002; Sobel 2003; Chou and Neelin 2004; Sobel and Neelin 2006; Chou et al. 2009; Harrop and Hartmann 2016; Popp and Silvers 2017; Dixit et al. 2018; Emanuel 2019). This energetic theory has been used to quantify the processes contributing to projected narrowing of the ITCZ in coupled climate models (Byrne and Schneider 2016b) and could potentially be applied to understand the observed ITCZ narrowing over recent decades (Wodzicki and Rapp 2016).

Despite these recent advances in our mechanistic understanding of ITCZ width, there are opportunities for further progress by considering the dynamics of the atmospheric boundary layer. The boundary-layer momentum budget has been successfully invoked to explain the spatial distribution of tropical low-level convergence and precipitation (Lindzen and Nigam 1987; Waliser and Somerville 1994; Tomas et al. 1999; Stevens et al. 2002; Sobel 2007; Gonzalez et al. 2016) but has not been applied specifically to the problem of ITCZ width. There has been a long-standing debate in the atmospheric dynamics community regarding whether tropical convergence is driven by boundary-layer dynamics or by thermodynamic processes higher in the atmosphere such as latent-heat release [see section 2 of Sobel and Neelin (2006) for a summary of these competing arguments]. Now there is a developing consensus that low-level convergence — and hence ITCZ width — is primarily controlled by surface pressure gradients and boundary-layer dynamics (Lindzen and Nigam 1987; Sobel and Neelin 2006; Back and Bretherton 2009). It is therefore important to develop an understanding of ITCZ width from a dynamics perspective to complement the recent studies based on energetics and thermodynamics (Chou et al. 2009; Byrne and Schneider 2016a; Harrop and Hartmann 2016; Popp and Silvers 2017; Dixit et al. 2018).

Here we use the boundary-layer zonal momentum budget together with idealized simulations to investigate the dynamics of ITCZ width. In particular, we examine the momentum budget near the ITCZ edge, assess the dominant terms, and quantify the processes controlling low-level convergence and vertical velocity in that region. We also derive a range of scalings for ITCZ width and assess the importance of Ekman vs non-Ekman processes. Finally, we link ITCZ width to sea-surface temperature (SST) and boundary-layer moist entropy using simple extensions to the theories of Lindzen and Nigam (1987) and Emanuel (1995).

2. Simulations

a. Idealized GCM

We perform simulations using the idealized, grey-radiation GCM of O'Gorman and Schneider (2008) based on the model developed by Frierson et al. (2006) and Frierson (2007). Insolation is set to an annual-mean profile and the longwave optical thickness is specified as a function of latitude and pressure. All the idealized simulations discussed here are run in an aquaplanet configuration with a mixed layer of depth 1m and no horizontal energy transports (zero q-fluxes). The aquaplanet configuration has no inter-hemispheric asymmetries in statistical steady state and consequently the ITCZ is centered on the equator. The model has a horizontal spectral resolution of T127, 20 vertical σ-levels and an integration timestep of 150 seconds. Simulations are spun up for 700 days with averages taken over the subsequent 1000 days. See Byrne and Schneider (2016a) for an extended description of the model setup.

In the set of simulations analyzed here, the longwave optical thickness is varied so as to mimic changes in greenhouse-gas concentrations. We analyze a suite of 11 simulations: The longwave optical thickness for each simulation is based on a reference profile that has been re-scaled by different factors α[1].

[1]For the idealized-GCM simulations we re-scale the longwave optical thickness of a reference simulation by the following factors: $\alpha = 0.4, 0.5, 0.7, 0.8, 1.0, 1.2, 1.5, 1.8, 2.0, 2.5, 3.0$.

b. CMIP5 models

We also examine ITCZ width in three fixed-SST aquaplanet simulations from the Coupled Model Intercomparison Project Phase 5 (CMIP5) (Taylor et al. 2012): *aquaControl*, *aqua4K* and *aqua4xCO2*. Simulations from the IPSL-CM5A-LR, CNRM-CM5, IPSL-CM5B-LR, FGOALS-g2, MIROC5, HadGEM2-A, MPI-ESM-MR, MRI-CGCM3, and MPI-ESM-LR climate models are analyzed.

3. Boundary-layer dynamics near the ITCZ edge

a. Definition of ITCZ width

We define ITCZ width as the degrees latitude between the northern and southern ITCZ edges. The edges of the ITCZ are defined as the latitudes closest to the equator (north and south) at which the time-mean vertical velocity at the boundary-layer top is zero. In the idealized-GCM simulations we specify the boundary-layer top as the $\sigma = 0.8$ level. This is similar to the definition of Byrne and Schneider (2016a) but in their analysis the mid-tropospheric mass streamfunction is used to define the ITCZ edges. We choose to focus on the boundary-layer ITCZ width because it is more directly connected to the boundary-layer momentum budget, which is the tool used here to investigate the ITCZ. In addition, rainfall is driven by low-level convergence and vertical velocity at the boundary-layer top, and so a boundary-layer definition of ITCZ width is expected to be more relevant for rainfall and the hydrological cycle. Although we will mostly focus on the boundary-layer definition of ITCZ width, in Section 4 we discuss how ITCZ widths based on boundary-layer vs mid-tropospheric definitions do not always behave similarly as climate in varied, and that the utility of dynamical scalings for ITCZ width can depend on the definition used.

b. ITCZ width vs global-mean SST in idealized-GCM simulations

The average ITCZ width across the set of simulations over which longwave optical thickness is varied is 9.6° latitude; the width varies by 4° as the global-mean SST is increased from 272 K to 306 K (Figure 1a). ITCZ width does not change monotonically with global warming in these idealized simulations, rather the ITCZ widens with warming in cooler climate and narrows with warming in hotter climates. Here we use boundary-layer dynamics to analyze these variations of ITCZ width with global-mean SST.

c. Zonal momentum budget

We start with the steady-state zonally-averaged zonal momentum equation [see Peixóto and Oort (1984)]:

$$fv = -F_x - \frac{\tan\phi}{a}uv + \frac{v}{a}\frac{\partial u}{\partial \phi} + \omega\frac{\partial u}{\partial p}, \tag{1}$$

where $f = 2\Omega\sin\phi$ is the Coriolis parameter, F_x is the zonal component of the frictional force, a is Earth's radius, ϕ is latitude in radians, ω is the vertical (pressure) velocity, and the other symbols have their usual meanings. Taking the mass-weighted vertical average over the boundary layer, equation (1) becomes:

$$\underbrace{f[v]}_{\text{Coriolis}} = \overbrace{-(g/\Delta p)\tau_{x,\mathrm{sfc}}}^{\text{frictional}} \underbrace{-\frac{\tan\phi}{a}[uv]}_{\text{metric}} + \overbrace{\left[\frac{v}{a}\frac{\partial u}{\partial \phi}\right]}^{\text{horiz. adv.}} + \underbrace{\left[\omega\frac{\partial u}{\partial p}\right]}_{\text{vert. adv.}}, \tag{2}$$

where $[\cdot]$ denotes a mass-weighted vertical average over the boundary layer, g is the acceleration due to gravity, $\Delta p = p_s - p_{\mathrm{BL}}$ is the pressure difference between the surface and the boundary-layer top, and $\tau_{x,\mathrm{sfc}}$ is the zonal component of the vertical turbulent stress (which we will call the zonal wind stress). The various forces have been labeled: Coriolis, frictional, metric and horizontal/vertical advection of relative momentum. In deriving (2), we have assumed that the turbulent stress vanishes at the boundary-layer top.

In the reference idealized-GCM simulation ($\alpha = 1.0$), the Coriolis and frictional terms dominate the zonal momentum budget in the vicinity of the ITCZ edge (Figures 1b and 2a). The vertical and horizontal momentum advection terms have similar magnitudes but both are substantially smaller than the Coriolis and frictional terms; the metric term is negligible (Figure 2a) and will not be discussed further. It is common to assume Ekman balance in the tropical atmospheric boundary layer, i.e. a balance between Coriolis and frictional forces (e.g., Lindzen and Nigam 1987; Emanuel 1995; Held 2001). This force balance holds approximately at the ITCZ edge across the wide range of climates simulated by the idealized GCM (Figure 1b), which suggests that Ekman balance is a natural starting point for understanding the dynamics of ITCZ width. A recent study found that Ekman balance breaks down near the ITCZ, at least in a dry equatorial β-plane model of the tropical boundary layer, because the horizontal-advection term becomes large (Gonzalez et al. 2016). In our idealized-GCM simulations we note that the vertical- and horizontal-advection terms become relatively more important at the ITCZ edge in warmer climates as the magnitudes of the Coriolis and frictional terms decrease (Figure 1b). However, the zeroth-order balance is between Coriolis and frictional accelerations across all idealized-GCM simulations.

In the boundary-layer momentum budget the frictional force provides an eastward acceleration to the zonal wind at the ITCZ edge because the tropical surface winds are easterly (Figure 2b); there is a transfer of zonal momentum from the surface to the overlying atmosphere. This eastward acceleration is largely balanced by westward acceleration associated with equatorward advection of air with relatively low planetary angular momentum by the surface branch of the Hadley cell (the Coriolis term). For all except the coldest two simulations (Figure 1b), both the vertical- and horizontal-advection terms provide a westward acceleration to the boundary-layer zonal wind at the ITCZ edge by advecting low-angular momentum air. The horizontal-advection term accelerates the easterly zonal wind at the ITCZ edge provided the maximum in tropical surface easterlies is poleward of the ITCZ edge, as is the case in the reference simulation (Figure 2b). Equivalently, if the latitude of zero surface relative vorticity (where $\partial u_{\mathrm{sfc}}/\partial\phi = 0$) lies poleward of the ITCZ edge, the horizontal advection term will accelerate the easterly zonal flow there. For the vertical-advection term, if the latitude at which the flow is non-divergent (i.e. where $\partial\omega/\partial p = 0$) did not vary with height, the vertical advection term in (2) would be identically zero at the ITCZ edge. However, the latitude of non-divergence does vary with height in the idealized-GCM simulations (not shown). Consequently the vertical advection term in the zonal momentum budget is non-zero and accelerates the easterly zonal wind for the majority of simulations (Figure 1b).

4. Scalings for ITCZ width based on Ekman balance

We have demonstrated that the boundary layer at the ITCZ edge is approximately in Ekman balance in the idealized GCM (Figure 1b). We now use Ekman balance to derive simple dynamical scalings for ITCZ width and apply these scalings to the idealized-GCM and CMIP5 simulations.

a. Relationship between ITCZ width, wind stress and vorticity

Perhaps the simplest estimate for the latitude of the ITCZ edge (and ITCZ width) is obtained by assuming Ekman balance in the atmospheric boundary layer and taking the wind stress to be linearly proportional to the surface wind (e.g., Held and Hou 1980):

$$f[v] = C u_{\mathrm{sfc}}, \tag{3}$$

where C is a constant drag coefficient. Combining (3) with the zonally-averaged mass continuity equation in pressure coordinates[2], assuming zero vertical velocity at the surface, and for now neglecting meridional variations in the Coriolis parameter, it is straightforward to show that vertical velocity at the top of the boundary layer (ω_{BL}) is proportional to the surface relative vorticity: $\omega_{\mathrm{BL}} \propto \partial u_{\mathrm{sfc}}/\partial\phi$. This relationship suggests that the ITCZ-edge latitude, where $\omega_{\mathrm{BL}} = 0$ by definition, scales with the latitude where $\partial u_{\mathrm{sfc}}/\partial\phi = 0$ and the surface flow transitions from cyclonic to anti-cyclonic relative vorticity.

Testing this simple prediction in the idealized GCM, we find that the latitude of zero relative vorticity does not scale monotonically with the ITCZ edge defined in terms of boundary-layer vertical velocity (black circles in Figure 3). This implies, perhaps not surprisingly, that frictional Ekman convergence alone — where we have also neglected the component due to meridional gradients in the reciprocal of the Coriolis parameter — cannot capture the behavior of ITCZ width over the full range of idealized-GCM simulations. Interestingly, there is a strong correlation between the latitude of zero relative vorticity and the ITCZ edge defined in terms of the mid-tropospheric streamfunction (red circles in Figure 3) though the latitude of zero relative vorticity tends to underestimate the ITCZ width. From a dynamics perspective, the variation of the ITCZ edge with height and the contrasting scaling relationships between different ITCZ-width definitions (Figure 3) is likely due to terms in the zonal momentum budget being more or less influential at different levels in the atmosphere — this is a question to be investigated in future work. What is clear is that surface relative vorticity is closely tied to ITCZ width in the mid-troposphere but the connection to ITCZ width at the top of the boundary layer is more complex.

Related to this simple estimate for the ITCZ-edge latitude, Tomas and Webster (1997) argue that the barrier between boundary-layer convergence and divergence in the tropics (which is the ITCZ

[2]The steady-state continuity equation written in pressure coordinates is: $\frac{1}{a\cos\phi}\frac{\partial}{\partial\phi}(v\cos\phi) + \frac{\partial\omega}{\partial p} = 0$.

edge by our boundary-layer definition) coincides with the zero contour of the vertical component of *absolute* vorticity, where absolute vorticity in the zonal mean is $\eta = f - \frac{1}{a}\frac{\partial u_{\mathrm{sfc}}}{\partial \phi}$. If the product of the Coriolis parameter and absolute vorticity is negative ($f\eta < 0$) this implies that the flow is inertially unstable; Tomas and Webster (1997) find evidence of such unstable regions close to the equator and find that they are associated with cross-equatorial advection of absolute vorticity by large pressure gradients at the equator. In our idealized-GCM simulations, however, there are no inter-hemispheric asymmetries and so there is no time-mean pressure gradient at the equator and the zero contour of absolute vorticity lies at the equator. Consequently, the Tomas and Webster (1997) theory cannot explain the off-equatorial ITCZ edges in our simulations.

A more complete description of Ekman balance that includes the GCM-simulated wind stress $\tau_{x,\mathrm{sfc}}$ but still neglects the meridional gradient of $1/f$, suggests that the ITCZ edge should scale with the latitude where the easterly wind stress maximizes, i.e. where $\partial \tau_{x,\mathrm{sfc}}/\partial \phi = 0$. The estimates of the ITCZ edge based on where wind stress maximizes are very similar to those based on the latitude of zero relative vorticity (Figure 3). This agreement indicates that, at least for the idealized-GCM simulations, the simplifying assumptions of linear drag and a constant drag coefficient are reasonable when investigating ITCZ width.

Figure 3 demonstrates that the surface wind stress alone cannot fully capture the dynamics of boundary-layer ITCZ width. Before considering how other terms in the momentum budget affect ITCZ width (specifically momentum advection), we first explore in more depth the implications of perfect Ekman balance for ITCZ width. In particular, we derive additional Ekman scalings for the ITCZ-edge latitude and perturbations to this latitude that account for meridional structure in the Coriolis parameter and give conceptual insights into the coupling between wind stress and ITCZ width.

b. An Ekman scaling for ITCZ width

Further insights into the relationship between ITCZ width and wind stress can be obtained by rearranging (8). In particular, making the small-angle approximation so that $f = 2\Omega \sin\phi \approx 2\Omega\phi$ (valid close to the equator), ignoring the meridional gradients of $\cos\phi$ and Δp, and noting that $\omega_{\mathrm{BL}}(\phi_{\mathrm{ITCZ}}) = 0$ by definition, we obtain an expression for the ITCZ-edge latitude (ϕ_{ITCZ}) assuming Ekman balance:

$$\phi_{\mathrm{ITCZ}}^{\mathrm{ekman}} = \tau_{x,\mathrm{sfc}}(\phi_{\mathrm{ITCZ}}) / \left.\frac{\partial \tau_{x,\mathrm{sfc}}}{\partial \phi}\right|_{\phi=\phi_{\mathrm{ITCZ}}}, \tag{4}$$

where all quantities on the right-hand side are evaluated at the ITCZ edge. The diagnostic scaling (4) suggests that the latitude of the ITCZ edge (in radians) is directly proportional to the wind stress and inversely proportional to the meridional gradient of the wind stress. Figures 4 and 5 show estimates of the ITCZ-edge latitude using (4) in the idealized-GCM and CMIP5 simulations. Clearly Ekman dynamics as encapsulated in (4) captures some of the behavior of ITCZ width across the idealized ($r = 0.81$) and CMIP5 simulations ($r = 0.83$) but the estimates depart from the simulated ITCZ edges. This discrepancy hints at the importance of other processes — we investigate these processes in Sections 5 and 6. Nevertheless, the strong correlations in Figures 4 and 5 highlight a robust link between ITCZ width and Ekman balance. Before examining non-Ekman processes, we first use a toy model of the tropical boundary layer to further elucidate the implications of Ekman balance for ITCZ width.

c. Impact of wind-stress perturbations on ITCZ width: investigations with a toy model

The diagnostic scaling (4) shows how, assuming Ekman balance, the ITCZ-edge latitude relates to the magnitude and gradient of the zonal wind stress. But how do *perturbations* in wind stress, for example due to changes in windspeed or surface roughness, impact ITCZ width? To develop intuition for how ITCZ width is controlled by the wind stress, consider a stylized, reference zonal wind stress profile: $\tau_{\text{ref}}(\phi) = v_{max} \times (f\Delta p/g)\sin 9\phi$ (Figure 6a). This wind stress is defined to be in Ekman balance with a reference boundary-layer meridional wind $v(\phi) = v_{max}\sin 9\phi$ (Figure 6b). We specify $v_{max} = -5$ m/s and $\Delta p = 100$ hPa. For these reference profiles, the magnitude of the meridional wind maximizes at 10°N; the ITCZ-edge latitude is shifted marginally equatorward (9.9°N) because of the $\cos\phi$ weighting when calculating convergence and vertical velocity (Figure 6c). The maximum wind stress is on the poleward side of the ITCZ edge at 12.9°N (Figure 6a) as is also the case in the idealized-GCM simulations (Figure 3). This displacement between the latitudes of maximum wind stress and ITCZ edge in the toy model is caused by meridional gradients in the reciprocal of the Coriolis parameter.

We now perturb the reference stress profile in three ways and assess how these perturbations affect the ITCZ width:

1. *Add/subtract a constant stress:* Adding a constant westerly wind stress of $0.03\,\text{N/m}^2$ at all latitudes shifts the ITCZ edge poleward relative to its reference position by 0.8°. Adding a constant easterly wind stress of $0.03\,\text{N/m}^2$ shifts the ITCZ edge equatorward by 1.3° (Figure 6a,b,c).

2. *Multiply/divide stress by a factor of 2:* Multiplying or dividing the wind stress by 2 does not shift the ITCZ edge (Figure 6d,e,f), despite the imposed changes in stress being substantially larger than in the previous case where we added a constant stress.

3. *Shift latitude of maximum stress:* Manipulating the reference stress profile so as to shift the latitude of maximum stress equatorward and poleward has a large, amplified effect on the ITCZ-edge latitude (Figure 6g,h,i). Specifically, shifting the stress maximum equatorward by

1.1° causes an ITCZ shift of 3.4°; shifting the stress maximum poleward by 1.3° shifts the ITCZ edge poleward by 2.7°.

The Ekman scaling (4) we derived above is diagnostic but can be extended to provide simple explanations for the contrasting responses of ITCZ width to the imposed changes in wind stress described above. First define a function $\gamma(\phi) = \phi \frac{\partial \tau_{x,\mathrm{sfc}}}{\partial \phi} - \tau_{x,\mathrm{sfc}}$ which, according to (4), is zero at the ITCZ edge under the assumption of Ekman balance. We are interested in how ITCZ width responds to an arbitrary wind-stress perturbation. Using a first-order Taylor expansion of the perturbed function $\gamma(\phi)$ [denoted $\gamma'(\phi)$] about the reference ITCZ-edge latitude, we can approximate the change in ϕ_{ITCZ} as:

$$\delta\phi_{\mathrm{ITCZ}} \approx -\gamma'(\phi_{\mathrm{ITCZ}}) / \left.\frac{\partial \gamma'}{\partial \phi}\right|_{\phi_{\mathrm{ITCZ}}}, \tag{5}$$

where ϕ_{ITCZ} is the reference ITCZ-edge latitude.

Now we use (5) to interpret the ITCZ-edge shifts in Figure 6. Adding a constant wind stress $\delta\tau$ changes the magnitude of $\tau_{x,\mathrm{sfc}}$ but not its meridional gradient, and so $\gamma'(\phi_{\mathrm{ITCZ}}) = -\delta\tau$ and $\left.\frac{\partial \gamma'}{\partial \phi}\right|_{\phi_{\mathrm{ITCZ}}} = \phi_{\mathrm{ITCZ}} \left.\frac{\partial^2 \tau_{x,\mathrm{sfc}}}{\partial \phi^2}\right|_{\phi_{\mathrm{ITCZ}}}$, resulting in an expression for the change in ITCZ width in response to a constant wind-stress perturbation:

$$\delta\phi_{\mathrm{ITCZ}} \approx \frac{1}{\phi_{\mathrm{ITCZ}}} \left.\frac{\delta\tau}{\partial^2 \tau_{x,\mathrm{sfc}} / \partial \phi^2}\right|_{\phi_{\mathrm{ITCZ}}} \quad \text{for } \tau'_{x,\mathrm{sfc}} = \tau_{\mathrm{ref}} + \delta\tau, \text{ where } \delta\tau \text{ is a constant.} \tag{6}$$

The expression (6) reveals that the ITCZ-edge shift is directly proportional to the perturbation stress $\delta\tau$, and inversely proportional to the curvature of the reference $\tau_{x,\mathrm{sfc}}$ profile. For the wind-stress profiles considered in this toy model (Figure 6a,d,g), the curvature term is positive in the vicinity of the ITCZ edge ($\partial^2 \tau_{x,\mathrm{sfc}} / \partial \phi^2 > 0$). Consequently, adding a westerly stress (e.g. through weakened surface easterlies) widens the ITCZ whereas adding an easterly stress narrows the ITCZ

(Figure 6c). This scaling of ITCZ width with wind stress is supported by the idealized-GCM simulations (Figure 7). The asymmetry in the magnitudes of ITCZ-width responses to adding a westerly vs an easterly stress perturbation (Figure 6a,b,c) is not captured by the first-order Taylor expansion used to derive (6), but could be investigated with a higher-order expansion.

We can also use (5) to understand how scaling the wind stress by a constant factor μ affects the ITCZ width. We assume again for simplicity that the atmospheric boundary layer is in Ekman balance. For this wind-stress perturbation it is straightforward to show that $\gamma'(\phi_{\mathrm{ITCZ}}) = 0$ and thus for non-zero curvature in $\tau_{x,\mathrm{sfc}}$ there is no change in ITCZ width (see Figure 6f):

$$\delta\phi_{\mathrm{ITCZ}} = 0 \;\text{ for }\; \tau'_{x,\mathrm{sfc}} = \mu\tau_{\mathrm{ref}}. \tag{7}$$

Simple analytical expressions for changes in ITCZ width due to shifting the latitude of maximum wind stress (Figure 6g,h,i) are not as straightforward as for the previous two cases though could be derived using (5). What is clear is that subtle shifts in the latitude of maximum stress can lead to amplified shifts in ITCZ edge and that, perhaps intuitively, the ITCZ narrows when the maximum in wind stress moves towards the equator and widens when it moves poleward.

5. Boundary-layer convergence: Ekman vs non-Ekman processes

As discussed, Ekman dynamics cannot fully capture the behavior for ITCZ width across all simulations and additional processes need to be considered. ITCZ width is defined as a function of vertical velocity at the top of the boundary layer: The influences of Ekman vs non-Ekman processes on ITCZ width can be decomposed by assessing their respective contributions to ω_{BL} near the ITCZ edge. To perform this decomposition, we first convert the zonal momentum budget (2) into an equation for boundary-layer mass convergence and vertical velocity.

Neglecting the metric term in (2), dividing across by the Coriolis parameter, taking the derivative with respect to latitude, combining with the continuity equation and again assuming $\omega = 0$ at the surface, we obtain the following expression for vertical velocity at the boundary-layer top:

$$\omega_{\mathrm{BL}} = \underbrace{-\frac{g}{a\cos\phi}\frac{\partial}{\partial\phi}\left(\frac{\tau_{x,\mathrm{sfc}}}{f}\cos\phi\right)}_{\omega_{\mathrm{ekman}}} + \overbrace{\frac{\Delta p}{a\cos\phi}\frac{\partial}{\partial\phi}\left(\frac{\cos\phi}{f}\left[\omega\frac{\partial u}{\partial p}\right]\right)}^{\omega_{\mathrm{vert}}} + \underbrace{\frac{\Delta p}{a\cos\phi}\frac{\partial}{\partial\phi}\left(\frac{\cos\phi}{f}\left[\frac{v}{a}\frac{\partial u}{\partial\phi}\right]\right)}_{\omega_{\mathrm{horiz}}}. \tag{8}$$

The total vertical velocity is split into three components: A component associated with frictional Ekman convergence (ω_{ekman}) and components related to vertical and horizontal advection of relative momentum (ω_{vert} and ω_{horiz}, respectively). The components of vertical velocity in the vicinity of the ITCZ edge are plotted as a function of latitude for the reference simulation in Figure 8. The sum of the three components is approximately equal to the simulated vertical velocity; the small differences are due to the metric and residual terms in the zonal momentum budget being neglected.

Although the Coriolis and frictional terms approximately balance one another in the zonal momentum budget (Figure 1b), Ekman balance is insufficient for accurately estimating vertical velocity close to and within the ITCZ (Figure 8). It is therefore clear why the latitude of the ITCZ edge cannot be fully understood through Ekman dynamics alone. The vertical and horizontal advection terms have a relatively weak influence on the zonal momentum budget near the ITCZ edge (Figure 2a), but it is the meridional gradient of $1/f$ times these advection terms which determines convergence [see equation (8)]. The advection components of the vertical velocity are non-negligible at the ITCZ edge where they contribute to low-level convergence and ascent (Figure 8). Interestingly, the vertical and horizontal advection terms in the zonal momentum budget at the ITCZ edge are strongly correlated with one another across the idealized-GCM simulations (Figure 9). The importance of vertical advection of momentum between the boundary layer and free troposphere for determining tropical surface winds has been discussed previously (Stevens et al. 2002; Back and Bretherton 2009) so it is not surprising that this process affects ITCZ width. The horizontal-advection component ω_{horiz} is comparable to the vertical-advection component ω_{vert} across the idealized-GCM simulations (Figure 10). This term in the zonal momentum budget is often neglected in studies of tropical dynamics (e.g., Lindzen and Nigam 1987) but its importance for shaping tropical convergence has been highlighted previously (Holton 1975; Gonzalez et al. 2016). There is Ekman-driven descent at the ITCZ edge in the reference simulation (Figure 8) and across all the idealized-GCM simulations (Figure 10). In the majority of simulations the vertical and horizontal advection terms drive convergence and ascent at the ITCZ edge (Figures 8 and 10) and thus tend to widen the ITCZ relative to a hypothetical boundary layer in perfect Ekman balance. Figure 8 shows that vertical and horizontal momentum advection are crucial for the spatial distribution of convergence and rainfall in the tropics — we will return to the influence of these advection processes on ITCZ width in the next section.

a. Influence of meridional gradients in the Coriolis parameter on ITCZ width

Vertical velocity is driven by components associated with meridional gradients in (i) zonal wind stress and momentum advection and (ii) the reciprocal of the Coriolis parameter (8). It is interesting to compare these components: Both are large near the ITCZ (compare the solid and dotted black lines in Figure 8), indicating that ITCZ width is controlled by a delicate balance between the two terms. Meridional structure in the reciprocal of the Coriolis parameter is of zeroth-order importance for ITCZ width; the strong gradient in this function close to the equator drives descent and therefore acts to narrow the ITCZ (Figure 8). The influence of the Coriolis parameter on boundary-layer convergence decays rapidly ($\sim 1/\tan\phi$) moving poleward away from the ITCZ.

6. Scaling for ITCZ width based on the full momentum budget

The magnitude and pattern of zonal wind stress, via its influence on frictional Ekman convergence, is a strong constraint on ITCZ width (Figures 4, 5 6 and 7). However, in the previous section we demonstrated that ITCZ width is controlled by convergence driven by wind stress and horizontal/vertical advection of momentum. Below we introduce a "full" dynamical scaling to quantitatively investigate these competing physical controls on ITCZ width.

It is difficult to cleanly assess the roles of Ekman vs non-Ekman processes in determining the ITCZ width by examining the components of vertical velocity (8). This is because the Ekman component does not pass through zero close to the equator in the idealized GCM and so an "Ekman-only ITCZ width" is not defined. To quantitatively compare the effects of Ekman vs non-Ekman processes on ITCZ width, we instead derive an extended version of the analytical scaling (4) for the ITCZ-edge latitude that includes horizontal and vertical advection of momentum:

$$\phi_{\mathrm{ITCZ}}^{\mathrm{full}} = \left. \frac{-(g/\Delta p)\tau_{x,\mathrm{sfc}} + \left[\omega \frac{\partial u}{\partial p}\right] + \left[\frac{v}{a}\frac{\partial u}{\partial \phi}\right]}{-(g/\Delta p)\frac{\partial \tau_{x,\mathrm{sfc}}}{\partial \phi} + \frac{\partial}{\partial \phi}\left[\omega \frac{\partial u}{\partial p}\right] + \frac{\partial}{\partial \phi}\left[\frac{v}{a}\frac{\partial u}{\partial \phi}\right]} \right|_{\phi=\phi_{\mathrm{ITCZ}}}, \tag{9}$$

where all quantities on the right-hand side are evaluated at the ITCZ edge. This "full" dynamical scaling (9) captures the ITCZ-edge latitude across the full range of idealized-GCM simulations with a correlation coefficient of $r = 0.96$ (Figure 4) and does reasonably well at capturing the behavior in more complex CMIP5 simulations ($r = 0.81$; Figure 5). For the idealized-GCM simulations, comparing the black and red circles in Figure 4 we find that neglecting the momentum advection terms leads to an error in estimating the ITCZ-edge latitude that is substantial (approximately 2° latitude) relative to the ITCZ width itself. Clearly momentum advection must be accounted for in any quantitative theory of ITCZ width. The role of momentum transport by transient eddies in controlling ITCZ width is illustrated by comparing the blue and black circles in

Figure 4. Neglecting vertical and horizontal momentum advection by transient eddies gives errors of approximately 1° in estimates of the ITCZ-edge latitude. This non-negligible influence of transient eddies on ITCZ width is consistent with Byrne and Schneider (2016a,b) who found, using an energetic framework, that transient eddies are a key process controlling ITCZ width.

7. Relationships between ITCZ width and surface temperature, moist entropy

Up to this point we have studied ITCZ width in terms of dynamical quantities, specifically wind stress and momentum advection. It is also useful [and somewhat traditional in the field of tropical atmospheric dynamics (Sobel 2007)] to construct theories connecting the circulation to surface thermodynamic quantities such as SST; below we propose two such theories for ITCZ width.

a. Lindzen-Nigam theory

Lindzen and Nigam (1987) argued that tropical surface winds and convergence are closely controlled by the SST distribution via its influence on boundary-layer pressure gradients. In order to make the problem more tractable and link surface winds directly to SST, Lindzen and Nigam (1987) neglected horizontal and vertical momentum advection and assumed that pressure gradients vanish above the boundary layer. Despite the validity of these assumptions being challenged (e.g., Battisti et al. 1999), observations suggest that surface convergence in the tropics is largely driven by pressure gradients within (rather than above) the boundary layer (Back and Bretherton 2009). This is a strong indication that SST gradients are dynamically tied to ITCZ width.

To make our discussion of the link between ITCZ width and SST more concrete, consider simplified forms of the zonal (10) and meridional (11) momentum equations in Ekman balance following Lindzen and Nigam (1987):

$$f[v] = C[u] \tag{10}$$

$$f[u] = -\left[\frac{1}{\rho a}\frac{\partial p}{\partial \phi}\right] - C[v]. \tag{11}$$

In equations (10) and (11) we have assumed for simplicity that the drag coefficient C is the same for zonal and meridional winds, and have formulated the frictional force in terms of the boundary-layer average winds. Combining the zonal and meridional momentum equations we obtain an expression for the meridional wind:

$$[v] = -\frac{C}{f^2 + C^2}\left[\frac{1}{\rho a}\frac{\partial p}{\partial \phi}\right]. \tag{12}$$

Ignoring pressure gradients above the boundary layer (which are typically taken to be small in the tropical free troposphere) and assuming that the boundary-layer temperature is tightly coupled to SST via turbulent surface heat fluxes, from (12) and the ideal gas law we expect the meridional wind to be proportional to the meridional SST gradient: $[v] \propto \partial SST/\partial\phi$. Neglecting gradients in $C/(f^2 + C^2)$, it follows that the low-level convergence and vertical velocity at the top of the boundary layer are proportional to the Laplacian (or curvature) of SST:

$$\omega_{\mathrm{BL}} \propto \frac{\partial^2 SST}{\partial \phi^2}. \tag{13}$$

If the relationship (13) holds, it suggests that the ITCZ-edge latitude should scale with the latitude where the Laplacian of SST is zero.

In the idealized-GCM simulations, there is reasonable agreement between the simulated ITCZ-edge latitudes and the latitudes where $\partial^2 SST/\partial\phi^2 = 0$ (Figure 11a), with a correlation coefficient of $r = 0.89$. The ITCZ-edge estimates from this adapted Lindzen-Nigam theory do not lie on the one-to-one line, and there are several reasons for this. Most importantly we have assumed

Ekman balance which, as discussed, cannot fully capture ITCZ width across the simulations. We have also assumed zero horizontal pressure gradients above the boundary layer and ignored vertical momentum transport, though these assumptions are not generally valid (Back and Bretherton 2009). Finally, we have neglected meridional gradients in the drag coefficient and Coriolis parameter. Nevertheless, the prediction from Lindzen-Nigam theory that the ITCZ-edge latitude should scale with the latitude where the Laplacian of SST is zero is found to approximately hold in idealized-GCM simulations and provides a simple framework for understanding ITCZ-width changes in response to changing SST patterns.

b. Emanuel (1995) theory

A complementary but distinct relationship between ITCZ width and surface temperature (and humidity) can be derived following Emanuel (1995). Emanuel considered the transition between an atmosphere in radiative-convective equilibrium (RCE) and an atmosphere with a thermally-direct overturning circulation. He found that a sufficient condition for the RCE state to breakdown and a circulation to emerge is for the meridional gradient in sub-cloud moist entropy to exceed a critical threshold. Beyond this critical threshold, thermal wind becomes inconsistent with Hide's theorem (Hide 1969) and a circulation spins up so as to reduce the meridional moist entropy gradient. Assuming active convection and moist adiabatic lapse rates, Emanuel derived an expression for this critical moist entropy gradient and further argued that tropical surface winds can be estimated by the degree to which the actual moist entropy distribution departs from the critical gradient. Shaw and Voigt (2016) applied this theory to understand shifts in the Hadley circulation and storm tracks under climate change, but it has not been applied to ITCZ width to our knowledge.

The Emanuel (1995) estimate for the balanced surface zonal wind is:

$$u_{\mathrm{sfc}} = \frac{SST - T_t}{fa} \frac{\partial}{\partial \phi}(s - s_{\mathrm{crit}}), \tag{14}$$

where T_t is the tropopause temperature (which we take to be the temperature at the $\sigma = 0.22$ level), $s = c_p \log \theta_e$ is the boundary-layer moist entropy, θ_e is the boundary-layer equivalent potential temperature and s_{crit} is the critical moist entropy distribution [see equation (7) of Shaw and Voigt (2016)]. Assuming Ekman balance, that $\tau_{x,\mathrm{sfc}} \propto u_{\mathrm{sfc}}$ and $u_{\mathrm{sfc}} \propto [u]$, and neglecting meridional gradients in $SST - T_t$ and the Coriolis parameter, we find:

$$\omega_{\mathrm{BL}} \propto \frac{\partial^2}{\partial \phi^2}(s - s_{\mathrm{crit}}). \tag{15}$$

Expressed in words, (15) suggests that the ITCZ width scales with the latitude where the Laplacian of the departure of moist entropy from its critical distribution is zero. This scaling holds to some extent in the idealized-GCM simulations when an outlier is excluded (Figure 11) suggesting that ITCZ width is dynamically coupled to surface temperature and specific humidity via atmospheric convection and angular-momentum constraints.

8. Summary

The dynamical processes controlling ITCZ width have been investigated using idealized simulations together with the boundary-layer zonal momentum budget and various scalings. In the simulations, Ekman processes place a strong constraint on ITCZ width: The boundary layer is approximately in Ekman balance (Figure 2a) and the Ekman component of vertical velocity is large at the ITCZ edge (Figure 8). Scalings for ITCZ width based on Ekman dynamics are useful for understanding the behavior of ITCZ width across simulations (Figures 3, 4, 5, 6 and 7). In particular, ITCZ width defined in terms of the mid-tropospheric streamfunction scales with the latitude where the surface *relative* vorticity is zero and the latitude where the meridional gradient in zonal wind stress is zero (Figures 3). However, the boundary-layer definition of ITCZ width does not scale with the latitude of zero relative vorticity — understanding why different metrics of ITCZ width do not generally scale with one another is a topic for future work.

Although the ITCZ edge scales with the latitude where the wind stress maximizes, the ITCZ edge robustly lies equatorward of the stress maximum due to meridional variations in the Coriolis parameter (Figures 3). An analytical Ekman scaling for the ITCZ-edge latitude (4) suggests that ITCZ width is directly proportional to the magnitude of the wind stress and inversely proportional to its meridional gradient. The link between wind-stress magnitude and ITCZ width is also found in the idealized-GCM simulations (Figure 7). The control of Ekman dynamics on ITCZ width is examined in more detail using a toy model of the atmospheric boundary layer (Figure 6). The ITCZ-width responses to simple wind-stress perturbations reveal non-intuitive behavior: Adding a constant westerly (easterly) wind stress widens (narrows) the ITCZ (Figure 6a,b,c). The size of the change in ITCZ width depends not only on the magnitude of the stress perturbation but also on the curvature of the reference stress profile. Multiplying a reference wind-stress profile by a constant factor does not shift the ITCZ edge (Figure 6d,e,f) but subtle changes in the latitude at which the wind stress maximizes lead to large shifts in the ITCZ edge (Figure 6g,h,i). Given that angular momentum imparted by the surface to the atmosphere in the tropics is transported poleward and ultimately returned to the solid Earth by the mid-latitude surface westerlies (e.g., Held 2000), it is clear that the dynamics of ITCZ width are connected to atmospheric circulations at higher latitudes (Watt-Meyer and Frierson 2019) and the problem is therefore inherently non-local.

Although Ekman processes are a primary influence on ITCZ width, a scaling which includes horizontal and vertical momentum advection [see equation (9)] is needed to quantitatively capture ITCZ width across the full range of idealized-GCM simulations (Figure 4). The magnitudes of the advection terms in the zonal momentum budget are small (Figure 2) but it is the meridional gradients of these terms that control vertical velocity and ITCZ width, and advection contributes substantially to vertical velocity at the ITCZ edge (Figure 8). Therefore a full, prognostic theory for ITCZ width requires not only a prediction for wind-stress changes but also for changes in horizontal and vertical momentum advection [though helpfully these advection terms are strongly correlated (Figure 9)].

Because of the fast timescales of atmospheric processes relative to the slow timescales on which ocean temperatures evolve, there has been a long-standing interest in developing theories for tropical circulation/precipitation given the SST distribution (e.g., Sobel 2007). Extending the Lindzen and Nigam (1987) theory we find, given a range of assumptions, that ITCZ width scales with the latitude at which the Laplacian of SST is zero (Figure 11). An alternative model of the tropical circulation (Emanuel 1995) suggests that ITCZ width scales with the latitude where the Laplacian of the departure of the boundary-layer moist entropy from a critical distribution is zero. Our extensions to the Lindzen and Nigam (1987) and Emanuel (1995) theories have some skill in capturing the behavior of ITCZ width across the idealized-GCM simulations.

The analyses and scalings presented here establish a dynamical framework with which to understand the processes determining ITCZ width. This dynamical framework complements recent efforts to understand ITCZ width based on the atmospheric energy budget (Chou et al. 2009; Byrne and Schneider 2016a; Harrop and Hartmann 2016; Dixit et al. 2018) and has the potential to be more informative and predictive, given that surface convergence and the ITCZ are driven predominantly by boundary-layer pressure gradients and dynamics rather than by thermodynamic effects higher in the atmosphere (Lindzen and Nigam 1987; Sobel and Neelin 2006; Back and Bretherton 2009). Our investigations into the dynamics of ITCZ width also advance fundamental understanding of the atmospheric circulation, and are likely to be useful for examining ITCZ biases in more complex climate models, differences in ITCZ width over land vs ocean regions, and the past and future evolution of tropical rainfall.

Acknowledgments. We acknowledge support from the Imperial College London Research Fellowship Scheme and useful discussions with David Battisti, Kerry Emanuel and Marty Singh. This work used JASMIN, the UK collaborative data analysis facility.

References

Back, L. E., and C. S. Bretherton, 2009: On the relationship between SST gradients, boundary layer winds, and convergence over the tropical oceans. *J. Climate*, **22**, 4182–4196.

Battisti, D. S., E. S. Sarachik, and A. C. Hirst, 1999: A consistent model for the large-scale steady surface atmospheric circulation in the tropics. *J. Climate*, **12**, 2956–2964.

Bischoff, T., and T. Schneider, 2014: Energetic constraints on the position of the intertropical convergence zone. *J. Climate*, **27**, 4937–4951.

Bretherton, C. S., and A. H. Sobel, 2002: A simple model of a convectively coupled Walker circulation using the weak temperature gradient approximation. *J. Climate*, **15**, 2907–2920.

Broccoli, A. J., K. A. Dahl, and R. J. Stouffer, 2006: Response of the ITCZ to Northern Hemisphere cooling. *Geophys. Res. Lett.*, **33**.

Byrne, M. P., A. G. Pendergrass, A. D. Rapp, and K. R. Wodzicki, 2018: Response of the intertropical convergence zone to climate change: Location, width, and strength. *Current Climate Change Reports*, **4**, 355–370.

Byrne, M. P., and T. Schneider, 2016a: Energetic constraints on the width of the intertropical convergence zone. *J. Climate*, **29**, 4709–4721.

Byrne, M. P., and T. Schneider, 2016b: Narrowing of the ITCZ in a warming climate: Physical mechanisms. *Geophys. Res. Lett.*, **43**, 11,350–11,357.

Byrne, M. P., and T. Schneider, 2018: Atmospheric dynamics feedback: concept, simulations and climate implications. *J. Climate*, **31**, 3249–3264.

Chiang, J. C. H., and A. R. Friedman, 2012: Extratropical cooling, interhemispheric thermal gradients, and tropical climate change. *Annu. Rev. Earth Planet. Sci.*, **40**, 383–412.

Chou, C., and J. D. Neelin, 2004: Mechanisms of global warming impacts on regional tropical precipitation. *J. Climate*, **17**, 2688–2701.

Chou, C., J. D. Neelin, C.-A. Chen, and J.-Y. Tu, 2009: Evaluating the “rich-get-richer” mechanism in tropical precipitation change under global warming. *J. Climate*, **22**, 1982–2005.

Dixit, V., O. Geoffroy, and S. C. Sherwood, 2018: Control of ITCZ width by low-level radiative heating from upper-level clouds in aquaplanet simulations. *Geophys. Res. Lett.*, **45**, 5788–5797.

Donohoe, A., J. Marshall, D. Ferreira, and D. McGee, 2013: The relationship between ITCZ location and cross-equatorial atmospheric heat transport: From the seasonal cycle to the Last Glacial Maximum. *J. Climate*, **26**, 3597–3618.

Donohoe, A., and A. Voigt, 2017: Why future shifts in tropical precipitation will likely be small: The location of the tropical rain belt and the hemispheric contrast of energy input to the atmosphere. *Climate Extremes: Patterns and Mechanisms*, **226**, 115–137.

Emanuel, K. A., 1995: On thermally direct circulations in moist atmospheres. *J. Atmos. Sci.*, **52**, 1529–1536.

Emanuel, K. A., 2019: Inferences from simple models of slow, convectively coupled processes. *J. Atmos. Sci.*, **76**, 195–208.

Frierson, D. M. W., 2007: The dynamics of idealized convection schemes and their effect on the zonally averaged tropical circulation. *J. Atmos. Sci.*, **64**, 1959–1976.

Frierson, D. M. W., I. M. Held, and P. Zurita-Gotor, 2006: A gray-radiation aquaplanet moist GCM. Part I: Static stability and eddy scale. *J. Atmos. Sci.*, **63**, 2548–2566.

Frierson, D. M. W., and Coauthors, 2013: Contribution of ocean overturning circulation to tropical rainfall peak in the Northern Hemisphere. *Nat. Geosci.*, **6**, 940–944.

Gonzalez, A. O., C. J. Slocum, R. K. Taft, and W. H. Schubert, 2016: Dynamics of the ITCZ boundary layer. *J. Atmos. Sci.*, **73**, 1577–1592.

Harrop, B. E., and D. L. Hartmann, 2016: The role of cloud radiative heating in determining the location of the ITCZ in aquaplanet simulations. *J. Climate*, **29**, 2741–2763.

Held, I. M., 2000: The general circulation of the atmosphere. Lecture notes from the Woods Hole Geophysical Fluid Dynamics Program.

Held, I. M., 2001: The partitioning of the poleward energy transport between the tropical ocean and atmosphere. *J. Atmos. Sci.*, **58**, 943–948.

Held, I. M., and A. Y. Hou, 1980: Nonlinear axially symmetric circulations in a nearly inviscid atmosphere. *J. Atmos. Sci.*, **37**, 515–533.

Hide, R., 1969: Dynamics of the atmospheres of the major planets with an appendix on the viscous boundary layer at the rigid bounding surface of an electrically-conducting rotating fluid in the presence of a magnetic field. *J. Atmos. Sci.*, **26**, 841–853.

Holton, J. R., 1975: On the influence of boundary layer friction on mixed rossby-gravity waves. *Tellus*, **27**, 107–115.

Kang, S. M., I. M. Held, D. M. W. Frierson, and M. Zhao, 2008: The response of the ITCZ to extratropical thermal forcing: Idealized slab-ocean experiments with a GCM. *J. Climate*, **21**, 3521–3532.

Kang, S. M., Y. Shin, and S.-P. Xie, 2018: Extratropical forcing and tropical rainfall distribution: energetics framework and ocean Ekman advection. *npj Climate and Atmospheric Science*, **1**, doi:10.1038/s41612-017-0004-6.

Lindzen, R. S., and S. Nigam, 1987: On the role of sea surface temperature gradients in forcing low-level winds and convergence in the tropics. *J. Atmos. Sci.*, **44**, 2418–2436.

O'Gorman, P. A., and T. Schneider, 2008: The hydrological cycle over a wide range of climates simulated with an idealized GCM. *J. Climate*, **21**, 5797–5806.

Peixóto, J. P., and A. H. Oort, 1984: Physics of Climate. *Reviews of Modern Physics*, **56**.

Philander, S. G. H., D. Gu, G. Lambert, T. Li, D. Halpern, N. C. Lau, and R. C. Pacanowski, 1996: Why the ITCZ is mostly north of the equator. *J. Climate*, **9**, 2958–2972.

Popp, M., and L. G. Silvers, 2017: Double and single ITCZs with and without clouds. *J. Climate*, **30**, 9147–9166.

Schneider, T., T. Bischoff, and G. H. Haug, 2014: Migrations and dynamics of the intertropical convergence zone. *Nature*, **513**, 45–53.

Shaw, T. A., and A. Voigt, 2016: What can moist thermodynamics tell us about circulation shifts in response to uniform warming? *Geophys. Res. Lett.*, **43**, 4566–4575.

Sobel, A. H., 2003: On the coexistence of an evaporation minimum and precipitation maximum in the Warm Pool. *J. Climate*, **16**, 1003–1009.

Sobel, A. H., 2007: Simple models of ensemble-averaged precipitation and surface wind, given the sea surface temperature. *The Global Circulation of the Atmosphere, edited by T. Schneider and A. H. Sobel*, 219–251.

Sobel, A. H., and J. D. Neelin, 2006: The boundary layer contribution to intertropical convergence zones in the quasi-equilibrium tropical circulation model framework. *Theor. Comput. Fluid Dyn.*, **20**, 323–350.

Stevens, B., J. Duan, J. C. McWilliams, M. Münnich, and J. D. Neelin, 2002: Entrainment, Rayleigh friction, and boundary layer winds over the tropical pacific. *J. Climate*, **15**, 30–44.

Su, H., and Coauthors, 2017: Tightening of tropical ascent and high clouds key to precipitation change in a warmer climate. *Nat. Communications*, **8**, doi:10.1038/ncomms15771.

Taylor, K. E., R. J. Stouffer, and G. A. Meehl, 2012: An overview of CMIP5 and the experiment design. *Bull. Amer. Meteor. Soc.*, **93**, 485–498.

Tomas, R. A., J. R. Holton, and P. J. Webster, 1999: The influence of cross-equatorial pressure gradients on the location of near-equatorial convection. *Quart. J. Roy. Meteor. Soc.*, **125**, 1107–1127.

Tomas, R. A., and P. J. Webster, 1997: The role of inertial instability in determining the location and strength of near-equatorial convection. *Quart. J. Roy. Meteor. Soc.*, **123**, 1445–1482.

Waliser, D. E., and C. Gautier, 1993: A satellite-derived climatology of the ITCZ. *J. Climate*, **6**, 2162–2174.

Waliser, D. E., and R. C. J. Somerville, 1994: Preferred latitudes of the intertropical convergence zone. *J. Atmos. Sci.*, **51**, 1619–1639.

Watt-Meyer, O., and D. M. W. Frierson, 2019: ITCZ width controls on Hadley cell extent and eddy-driven jet position, and their response to warming. *J. Climate*, doi:10.1175/JCLI-D-18-0434.1, in press.

Wodzicki, K. R., and A. D. Rapp, 2016: Long-term characterization of the Pacific ITCZ using TRMM, GPCP, and ERA-Interim. *J. Geophys. Res.: Atmos.*, **121**, 3153–3170.

LIST OF FIGURES

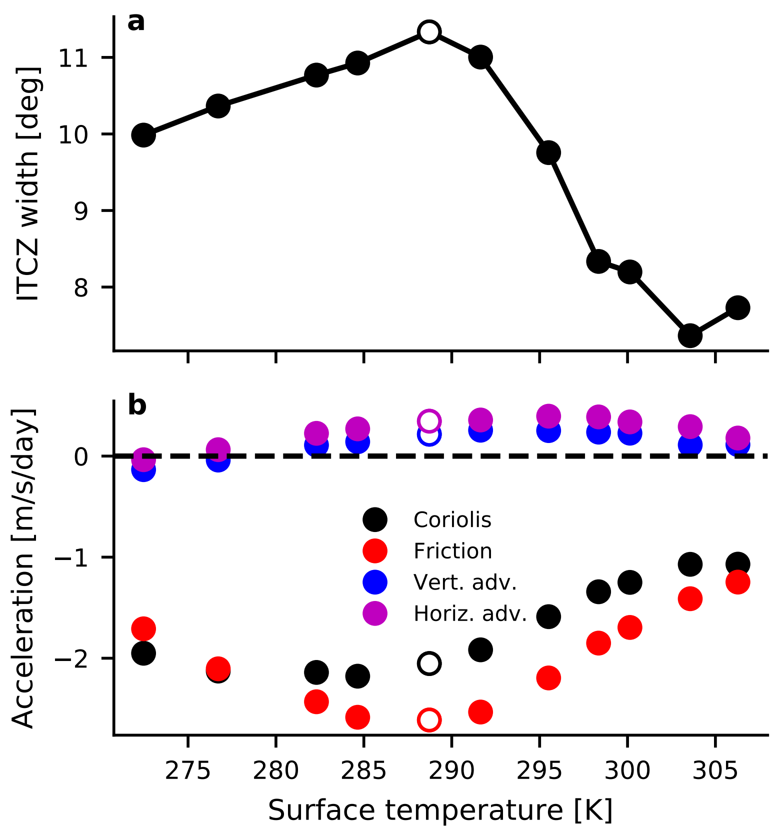

FIG. 1. (a) ITCZ width and (b) the various terms in the boundary-layer zonal momentum budget (2) evaluated at the northern ITCZ edge vs global-mean surface temperature for the idealized-GCM simulations with different longwave optical thicknesses. The ITCZ edges are defined as the latitudes closest to the equator (north and south) where the vertical velocity at the top of the boundary layer is zero. Here and in subsequent figures unfilled circles denote the reference simulation with a scaling factor of $\alpha = 1.0$ for the longwave optical thickness.

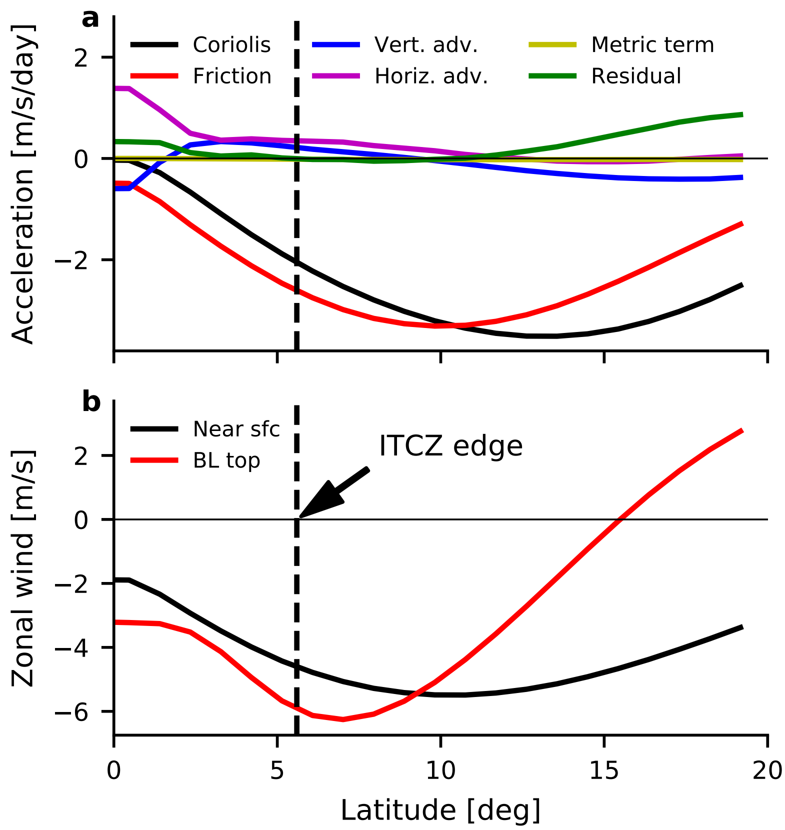

680 FIG. 2. (a) Terms in the boundary-layer zonal momentum budget (2) for the reference simulation ($\alpha = 1.0$). The solid black line is the Coriolis term, the red line is the friction term, blue is the vertical advection term, magenta is the horizontal advection term, yellow is the metric term and green is the budget residual. (b) Near-surface zonal wind ($\sigma = 0.98$; solid black line) and zonal wind at the boundary-layer top ($\sigma = 0.8$). For panels (a) and (b), the vertical dashed black lines indicate the northern edge of the ITCZ.

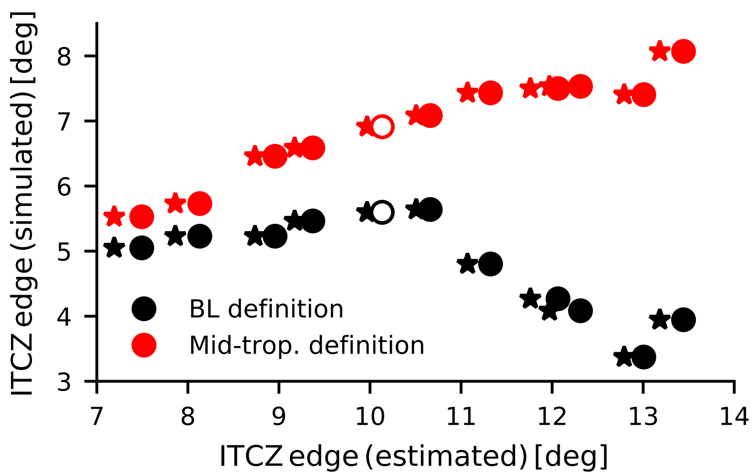

FIG. 3. Northern latitudes of the ITCZ edges in the idealized-GCM simulations vs the ITCZ edges estimated as the latitudes where $\partial u_{\mathrm{sfc}}/\partial\phi = 0$ (circles) and the latitudes where $\partial \tau_{x,\mathrm{sfc}}/\partial\phi = 0$ (stars). For the simulated ITCZ edges (y-axis), black markers show the edges defined in terms of vertical velocity at the top of the boundary layer and red markers show the edges defined using an alternative definition based on the mid-tropospheric streamfunction. Specifically, the streamfunction definition calculates the ITCZ edges as the latitudes north and south of the equator at which the streamfunction maximizes.

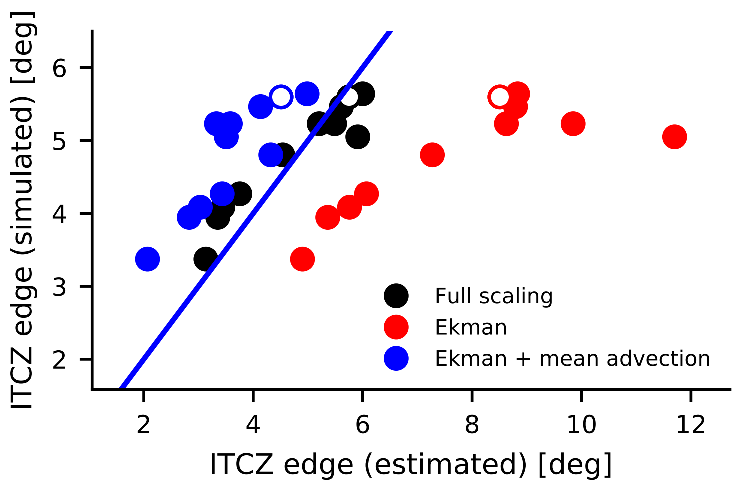

FIG. 4. Northern latitudes of the ITCZ edges vs estimates of these latitudes using scalings (4) and (9). The black circles indicate the full scaling (9) and the red circles show the estimates assuming Ekman balance (4), i.e. excluding horizontal and vertical momentum advection. The blue circles show estimates from the full scaling (9) but including only the time-mean contributions to the advection terms (excluding the transient-eddy contributions). The transient-eddy contributions to momentum advection are estimated using 6-hourly model data. Smoothing is applied to the meridional gradients of the wind-stress and advection terms prior to evaluating the scalings. Here and in subsequent figures, the blue line indicates a one-to-one relationship.

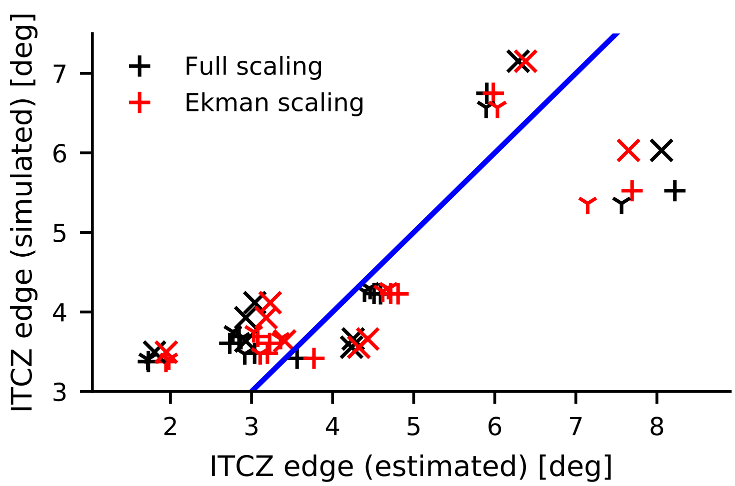

698 FIG. 5. As in Figure 4 but here showing the simulated and estimated latitudes of the northern ITCZ edges
699 in CMIP5 simulations. The pluses, crosses and triangles indicate the *aquaControl*, *aqua4K* and *aqua4xCO2*
700 simulations, respectively.

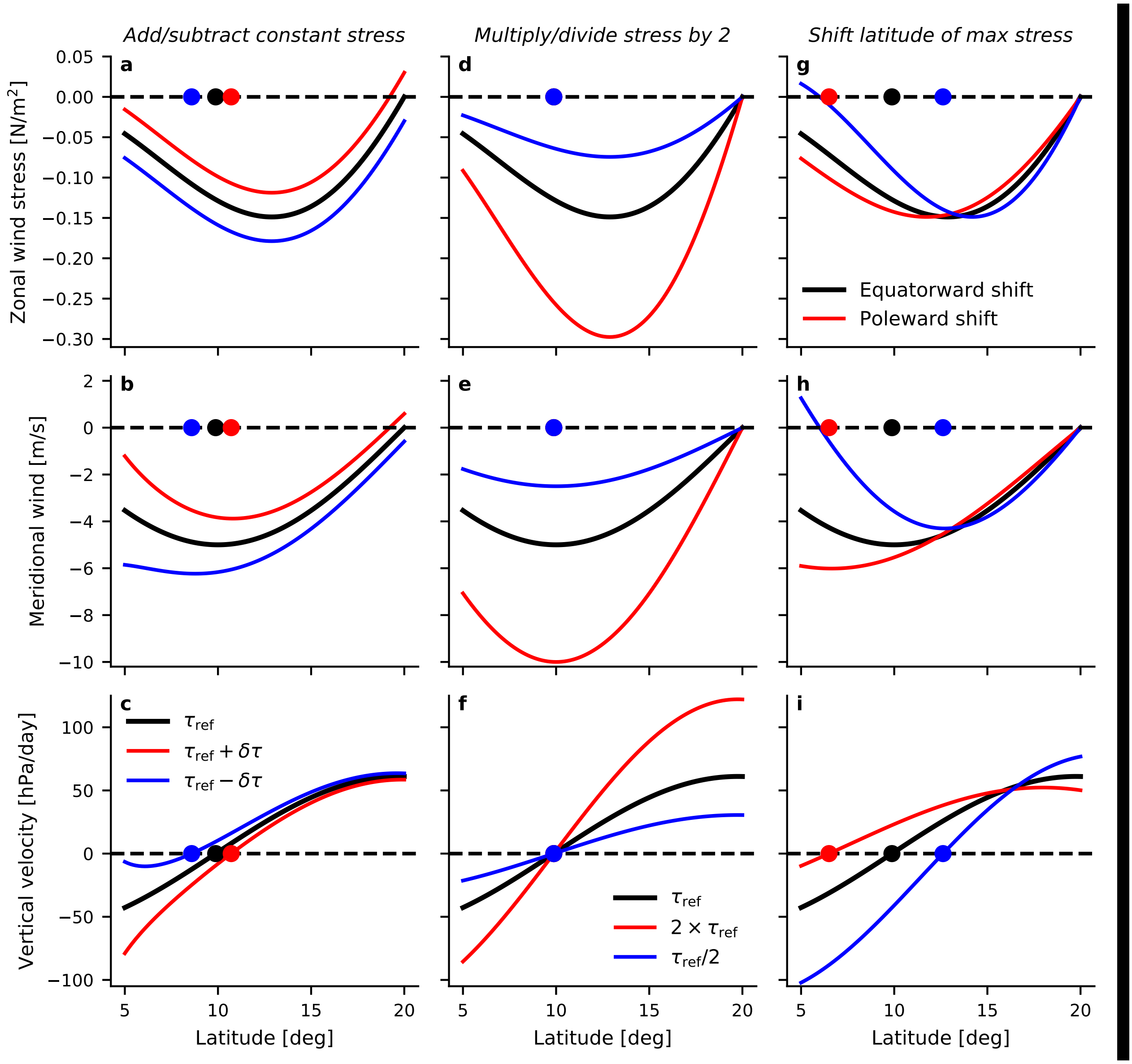

FIG. 6. (a,d,g) Zonal wind stress, (b,e,h) meridional wind in the boundary layer and (c,f,i) vertical velocity at the top of the boundary layer in a toy Ekman model of the tropical atmosphere. The solid black lines denote the reference wind stress, meridional wind and vertical velocity profiles. In each column different perturbations have been applied to the reference stress profile: In panels (a,b,c) a constant westerly stress has been added (red lines) and subtracted (blue lines), in panels (d,e,f) the reference stress has been multiplied (red lines) and divided (blue lines) by a factor 2, and in panels (g,h,i) the latitude of maximum stress has been shifted equatorward (red lines) and poleward (blues lines). The colored circles show the latitudes of the ITCZ edges for the corresponding stress profiles, where the ITCZ edge is defined as the latitude at which the vertical velocity at the top of the boundary layer is zero.

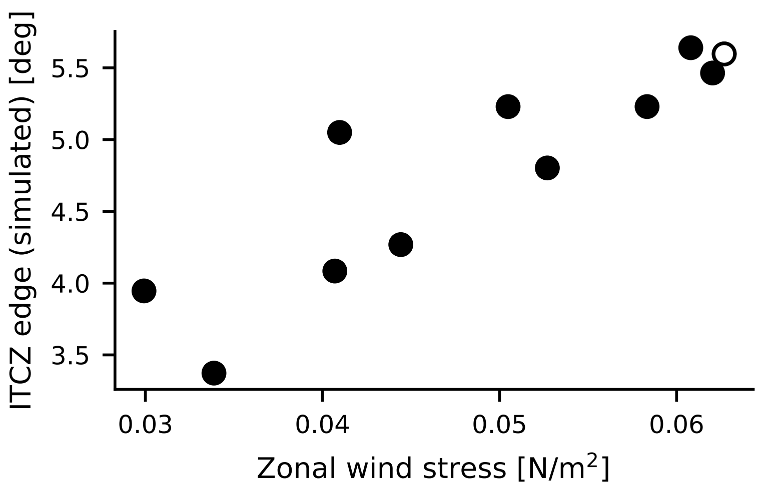

710 FIG. 7. Latitude of the northern edge of the ITCZ vs the zonal wind stress at the ITCZ edge in the idealized-
711 GCM simulations.

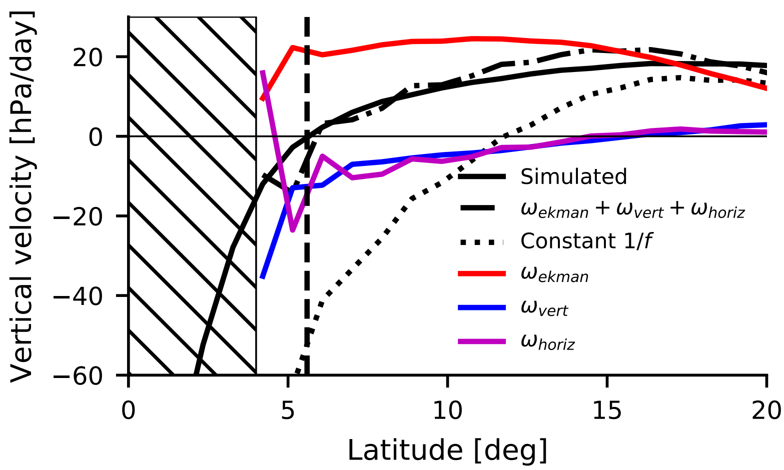

FIG. 8. Vertical velocity at the top of the boundary layer ($\sigma = 0.8$) for the reference simulation (solid black line). Also shown are the Ekman (red line), vertical-advection (blue line), and horizontal-advection (magenta line) components of the vertical velocity as defined by (8), along with their sum (dashed-dotted black line). The dotted black line shows an estimate of vertical velocity for which meridional gradients in the reciprocal of the Coriolis parameter have been neglected. The vertical dashed black line indicates the northern ITCZ edge. Note that the hatched region close to the equator does not show the estimated vertical-velocity components; at these latitudes the $1/f \sim 1/\phi$ dependence causes each component to rapidly increase in magnitude as $\phi \to 0$.

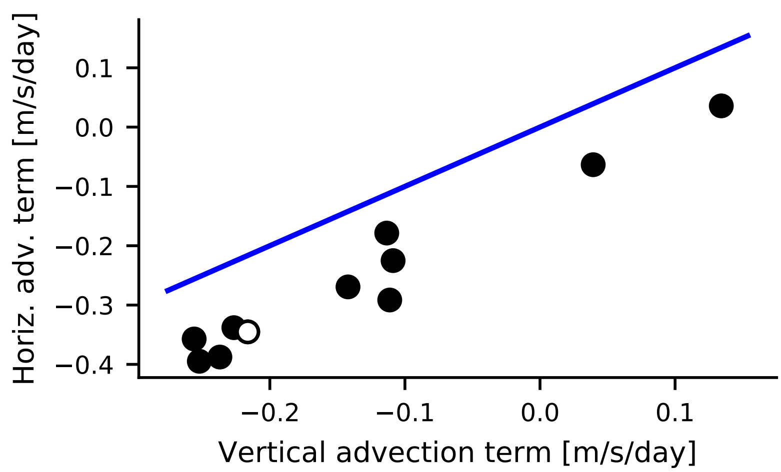

719 FIG. 9. Horizontal vs vertical momentum advection terms in the zonal momentum budget (2), evaluated at
720 the ITCZ edge for each idealized-GCM simulation.

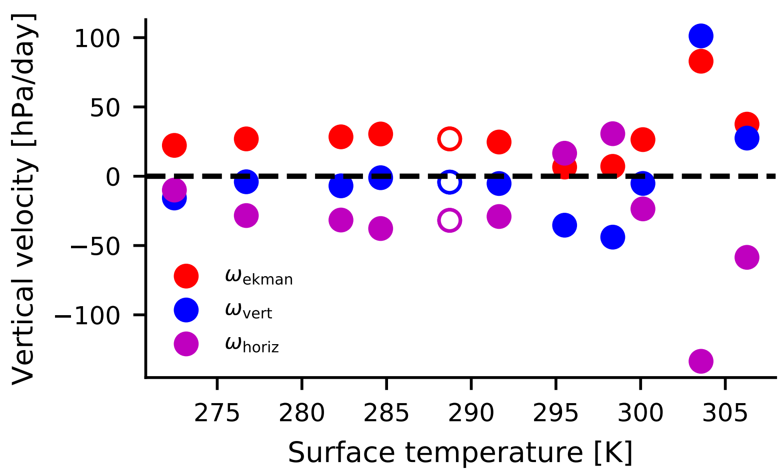

721 FIG. 10. Components of vertical velocity at the top of the boundary layer ($\sigma = 0.8$) at the ITCZ edge vs
722 global-mean surface temperature for the idealized-GCM simulations.

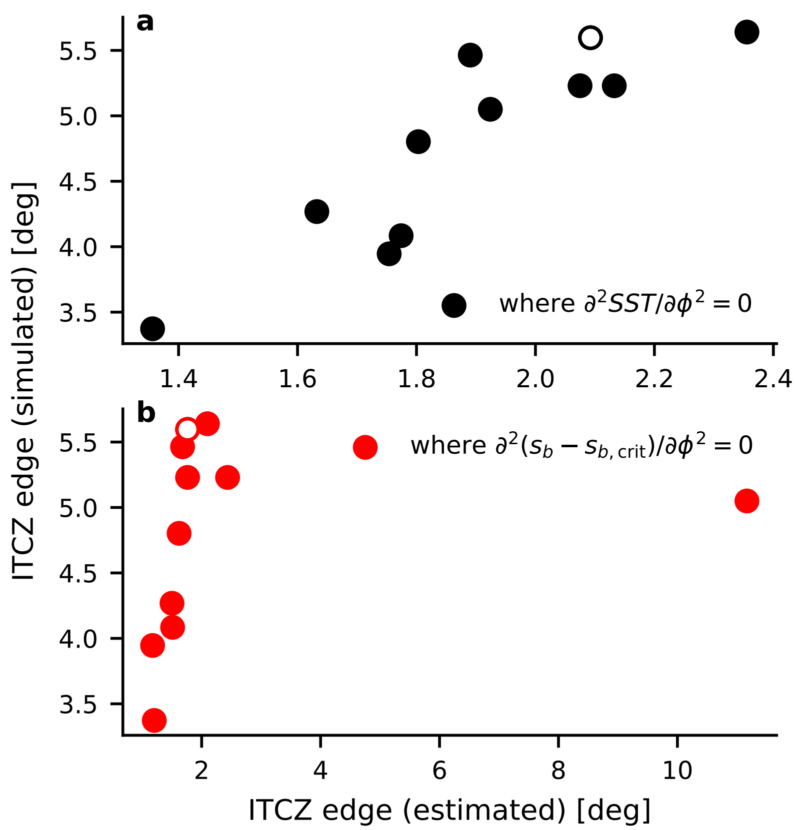

FIG. 11. Northern ITCZ edges in the idealized-GCM simulations vs the edges estimated as the latitudes closest to the equator where (a) the Laplacian of SST is zero and (b) the Laplacian of the departure of the simulated surface moist entropy distribution from the critical distribution is zero. See equations (13) and (15) for details. The correlation coefficients are $r = 0.89$ and $r = 0.21$ for panels (a) and (b), respectively. The correlation coefficient for (b) increases to $r = 0.77$ when the outlier is excluded.